

## ORIGINAL MILLIMETER-WAVE ANTENNAS WITH QUASI-GAUSSIAN RADIATION PATTERNS

Ronan SAULEAU, and Barbara CHANTRAINE-BARES

Institut d'Electronique et de Télécommunications de Rennes (IETR) – UMR CNRS 6164  
Université de Rennes 1, Campus de Beaulieu, Av. du Général Leclerc, 35042 Rennes Cedex – France  
*Ronan.Sauleau@univ-rennes1.fr*

### 1. Introduction

Millimeter-wave applications, such as 60 GHz high data-rate indoor communications systems or primary feeds of Focal Array Fed Reflectors operating in Q-band for next generation of multimedia satellites, may require reduced-size antennas with symmetrical (or not) quasi-gaussian radiation patterns.

This paper reports the design rules and characteristics of original antennas satisfying these requirements. They are fed by conventional printed primary sources whose radiation is shaped using either (i) Fabry-Perot cavities with uniform or non-periodic highly reflecting mirrors (section 2), or (ii) arbitrarily shaped homogeneous 3D dielectric lenses (section 3).

### 2. Directive Fabry-Perot Antennas

Electromagnetic bandgap (EBG) materials are dispersive and anisotropic periodic structures composed of metallic and/or dielectric elements that can prevent the propagation of electromagnetic radiation in one-dimensional (1-D), 2-D or 3-D directions. They behave simultaneously as frequency and spatial filters operating in the effective medium regime (in which the periodicity is small relative to the wavelength), or in the Bragg regime (where the periodicity is an appreciable amount of the wavelength, and constructive and destructive interference occurs) [1,2].

In particular, pioneer works of Ortusi *et al.* [3] and von Trentini [4], and more recent demonstrations, *e.g.* [5-8], have shown that resonant cavities of the Fabry-Perot (FP) type (with partially reflective surfaces (PRS) or Bragg mirrors) allow a significant reduction of the angular range of radiated fields, resulting in directive antennas.

The typical configuration of the antennas studied here is depicted in Fig. 1a. It consists of a FP cavity (of diameter  $\phi$  and central thickness  $D$ ) excited by an arbitrary printed primary source through a dielectric coupling region ( $\epsilon_{r,3}$ ,  $\tan\delta_3$ ) of thickness  $L$ . The cavity operates around its first maximum of transmission ( $D \approx \lambda_0/2 \sqrt{\epsilon_{r,4}}$ ). It comprises two highly reflecting metal mesh mirrors ( $M_1$  and  $M_2$ ) printed on a plano-convex (radius of curvature  $R_0$ ) or plane-parallel ( $R_0 = \infty$ ) low-loss substrate ( $\epsilon_{r,4}$ ,  $\tan\delta_4$ ).

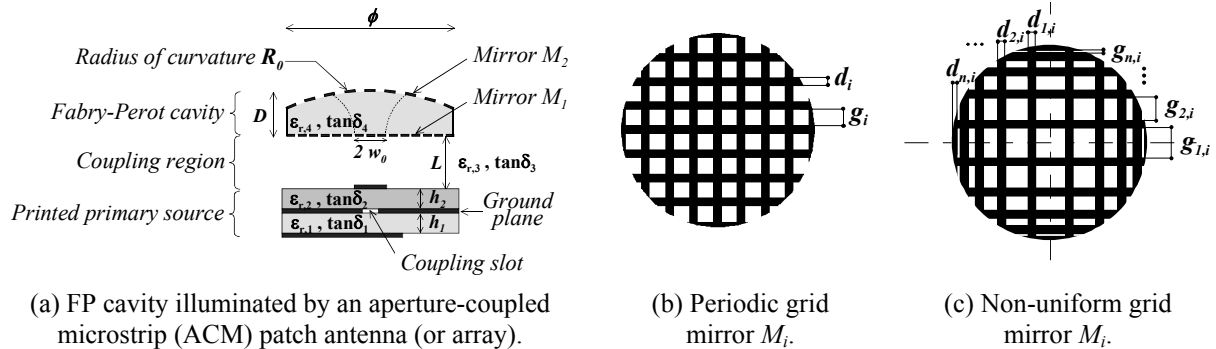
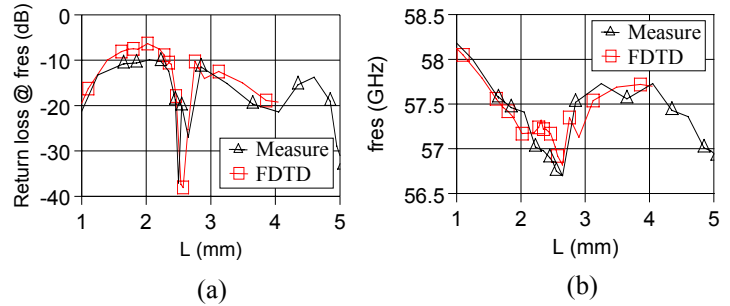


Fig. 1

In the *plano-convex* case, both mirrors are preferentially 2D inductive periodic meshes (Fig. 1b). Furthermore, the theoretical radiation patterns are perfectly gaussian [9], by analogy with dielectric loaded open resonators. Their directivity mainly depends on the waist size  $w_0$  of the beam (*i.e.* on  $R_0$ ). Similar performance can be obtained using *plane-parallel* FP resonators whose output mirror is a non-uniform PRS [10] (Fig. 1c). The same concept can be implemented for other beam shaping applications [11]. The input impedance and radiation performance of these two alternative configurations are investigated theoretically and experimentally in the 60 GHz band.

*Input impedance and mutual coupling:* to improve the radiation characteristics, it has been shown that the optimum value of  $L$  is around  $\lambda_0/2$  ( $\approx L_{opt}$ ) for a free-space coupling region ( $\epsilon_{r,3}=1$ ). On the other hand, the primary feeds used in most of the previous experiments [5-8] are simple radiating structures such as patch antennas, dipoles or monopoles. In this case, the input impedance and resonant frequency are very sensitive to any variation of  $L$  (especially around  $L_{opt}$ ), as illustrated in Fig. 2.

To our knowledge, no attempt has been carried out to reduce this sensitivity, which would be desirable from a practical viewpoint. A solution consists in exciting the resonator using a primary source with a moderate directivity ( $\sim 11$ -13 dB). This is clearly demonstrated in Fig. 3 where we compare the theoretical (FDTD) return loss at resonance of a cavity excited either by an ACM patch antenna, or by a  $2 \times 2$  elements ACM antenna array. This statement is confirmed experimentally in Fig. 4 where four antenna configurations are considered: the reflection coefficient  $r_e$  remains lower than  $-14$ dB (VSWR $<1.5$ ) for  $2.1\text{mm} < L < 2.6\text{mm}$  ( $\Delta L \approx 0.5\text{mm}$ ) if the FP cavity is illuminated by an ACM array (feed#2), whereas  $\Delta L \approx 0.2\text{mm}$  for feed#1 (ACM patch antenna).



**Fig. 2:** Variations of the measured and computed return loss at resonance (a), and resonant frequency (b), as a function of  $L$ . The cavity ( $\epsilon_{r,4}=3.80$ ,  $\tan\delta_4 \approx 10^{-4}$ ,  $\phi=20\text{mm}$ ,  $D=1284\mu\text{m}$ ,  $d_1=d_2=450\mu\text{m}$ ,  $g_1=g_2=450\mu\text{m}$ ) is fed by a single-layer patch antenna printed on a fused quartz substrate ( $\epsilon_r=3.80$ ,  $\tan\delta=5 \times 10^{-4}$ ,  $h=150\mu\text{m}$ ,  $W \times L=1972\mu\text{m} \times 1306\mu\text{m}$ ).

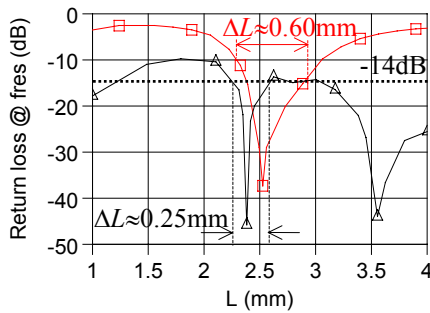


**Fig. 3:** Theoretical return loss at resonance. The FP cavity is excited by an ACM patch antenna ( $\triangle$ ) or by a  $2 \times 2$  elements ACM array ( $\square$ ).

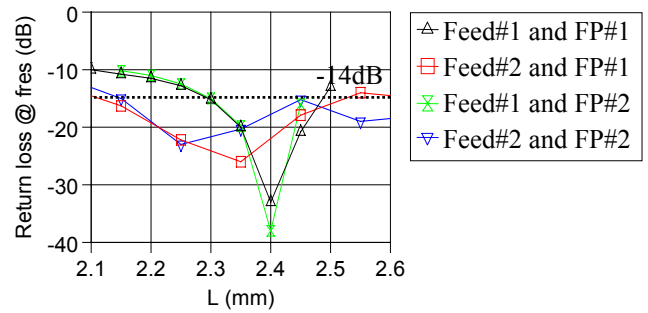


**Fig. 4:** Measured return loss at resonance. Four combinations of primary feeds and cavities are considered.  $Q_{FP\#1}=164$ ,  $Q_{FP\#2}=300$ .

*Radiation performance:* the radiation patterns and efficiencies of antennas based on *plano-convex* FP cavities have been discussed elsewhere as a function of (i) the coupling distance  $L$ , the  $Q$ -factor of the cavity (*i.e.* its directivity) and (iii) the topology of the primary feed [12]. Similar characteristics can be obtained using *plane-parallel* resonators whose mirror  $M_2$  behaves as a meta-film simulating a continuous spherical equiphase surface. This assumption is only valid in the long-wavelength regime ( $\max(g_{j,i}+d_{j,i}) \ll \lambda_0$ ,  $\forall i=1,2$  and  $j=1,\dots,n$ ). The dimensions of  $M_2$  are determined locally so that the phase of the internal reflection coefficient on  $M_2$  follows the spherical law governed by the beam waist size  $w_0$ , *i.e.* the directivity ( $\theta_{3\text{dB}} \approx 2\sqrt{\ln\sqrt{2}} \lambda_0 / (\pi w_0)$ ) of the antenna. A prototype operating at 57.6 GHz is shown in Fig. 5. It is excited by the same patch antenna as in Fig. 2. Its far-field radiation patterns in E- and H-planes are given in Fig. 6 for  $L=2.27 \pm 0.05\text{mm}$ . The FP cavity is in fused quartz ( $\epsilon_{r,4}=3.80$ ,  $\tan\delta_4 \approx 10^{-4}$ ,  $\phi=30\text{mm}$ ,  $D=1.266\text{mm}$ ,  $d_1=247\mu\text{m}$ ,  $g_1=353\mu\text{m}$ ,  $d_{j,2}+g_{j,2}=600\mu\text{m} \forall j$ ) and has an equivalent radius of curvature equal to 2595mm. The agreement between the measured and computed co-polar components is very satisfactory in the paraxial region, especially in H-plane. The gain has been measured by the comparison method with a standard gain horn in V-band. Its maximum value equals to 17.3 dB at resonance ( $D_0=21.2$  dB,  $\eta=41\%$ ). The total losses (3.9 dB) are due to the losses in the printed source (0.9 dB,  $\eta_{\text{feed}}=81\%$ ) and to the insertion losses of the cavity (3dB,  $\eta_{\text{FP}}=50\%$ ).

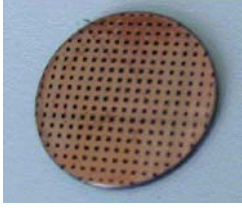


Fig. 5: FP cavity with a non-uniform grid mirror.

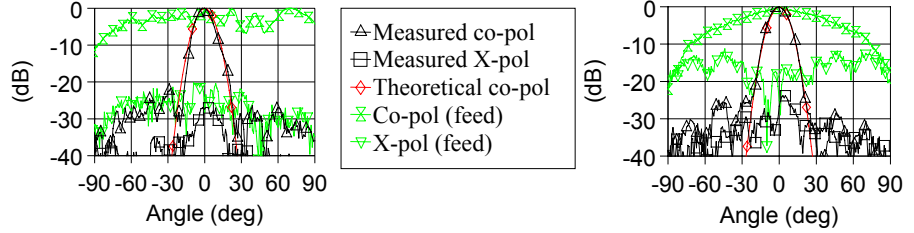


Fig. 6: Measured and computed (complex source-point method) radiation patterns in E-plane (left) and H-plane (right) at 57.6 GHz.

### 3. Arbitrarily shaped dielectric lens antennas

Specific broadband indoor communications scenarios may require shaping the radiation patterns of the antennas in order to optimize the cell coverage. It has been demonstrated that lens antennas are possible candidates for base-stations and mobile terminals [13]. In that work, an approximate lens profile is determined by applying, in several cut planes, the same design principles as for axis-symmetric lenses. We propose here to solve rigorously the synthesis problem of arbitrarily shaped 3D homogeneous dielectric lenses fed by printed antennas.

#### Synthesis of the lens profile and algorithm:

Fig. 7 depicts an arbitrary 3D lens (dielectric constant  $\epsilon_{r,d}$ ) fed by a punctual feed located at the origin  $O$ . The lens profile  $r(\theta, \phi)$  is computed using Geometrical Optics (GO) principles in order to obtain a desired far-field power pattern  $h(\alpha, \beta)$ , given the primary feed radiation pattern  $g(\theta, \phi)$ ;  $(\theta, \phi)$  and  $(\alpha, \beta)$  define the directions of the incident and refracted rays respectively. Application of the power conservation law and Snell's relations at the dielectric / air boundary enables to derive the following partial differential equation of the 2<sup>nd</sup> order in  $r$  [14]:

$$r_{\theta\theta}r_{\phi\phi} - r_{\theta\phi}^2 - a r_{\theta\theta} - b r_{\theta\phi} - c r_{\phi\phi} - H = 0 \quad (1)$$

This equation is strongly non-linear and is of the Monge-Ampere (M.A) type.  $r_{\theta}$  (resp.  $r_{\phi}$ ) represents the first (resp. second) partial derivative of  $r$  in  $\theta$  (resp. in  $\theta$  and  $\phi$ ). The coefficients  $a, b, c$  and  $H$  depend on  $\theta, \phi, r, r_{\theta}, r_{\phi}$ , and  $\epsilon_{r,d}$ . Their analytical expressions are given in [15]. Equation (1) is solved by successive iterations after linearization using second order centered finite differences [15,16]. This procedure enables to determine the lens profile  $r(\theta, \phi)$  with a given accuracy for any power patterns  $h(\alpha, \beta)$  and  $g(\theta, \phi)$ . The algorithm will be presented in details during the Conference.

*Computed and experimental results:* The synthesis procedure described above has been implemented to design a lens antenna radiating an asymmetric gaussian pattern at 58.5 GHz (the half-power beamwidth equals  $10^\circ$  in H-plane ( $\beta=0^\circ$ ) and  $30^\circ$  in E-plane ( $\beta=90^\circ$ )). The lens is excited by a microstrip  $2 \times 2$  patch antenna array printed on a RT\Duroid 5880 substrate ( $127\mu\text{m}$ ,  $\epsilon_r=2.23$ ,  $\tan\delta=0.004$ ) and fed by a V-type coaxial probe. The lens shape has been obtained after twelve iterations, starting from a half sphere ( $r=e$ ) as initial profile. Its central thickness ( $e=5.3\text{cm} \approx 10 \times \lambda_0$ ) is large enough to apply GO principles. Fig. 8 and 9 represent two cross-section views of the lens and the manufactured prototype in Teflon ( $\epsilon_{r,d}=2.23$ ).

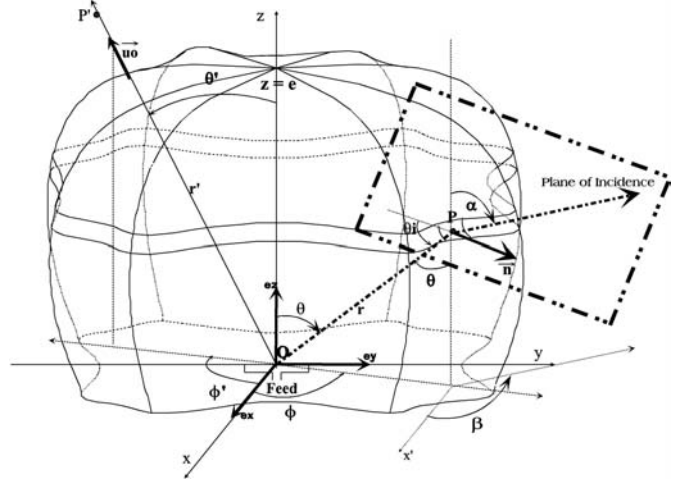


Fig. 7: Lens geometry.

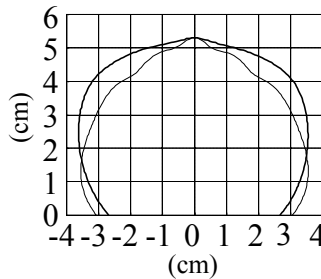


Fig. 8: Cross-section views of the lens.

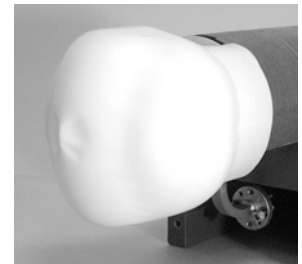


Fig. 9: 3D lens in Teflon.

Fig. 8 and 9 represent two cross-section views of the lens and the manufactured prototype in Teflon ( $\epsilon_{r,d}=2.23$ ).

The far-field radiation patterns (Fig. 10) of the lens antenna are computed using a classical hybrid approach combining GO and Physical Optics (PO). In E-plane, comparison with the measured patterns is satisfactory. The small dip observed in the broadside direction and the asymmetry of the main lobe are due to the actual radiation pattern of the primary source whose measurements through an hemisphere in Teflon slightly differs from the theoretical pattern  $g(\theta, \phi)$ . The -11dB side lobes observed in H-plane confirm the limitations of an approach only based on GO principles. Optimizing the lens profile (using a PO approach) enables to reduce significantly the side lobe level and reach the requirements [15].

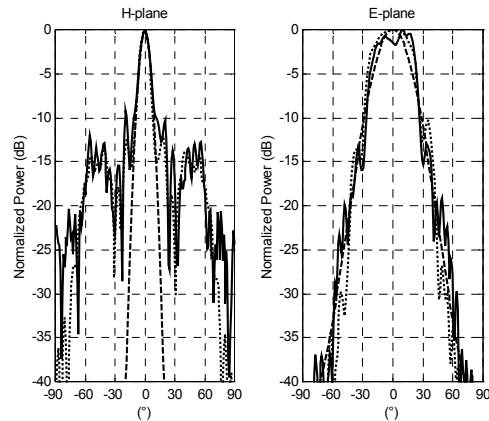


Fig. 10: Measured (—), computed (.....) and desired (---) radiation patterns at 58.5 GHz.

#### 4. Conclusion

Two kinds of original antennas with quasi-gaussian radiation patterns have been presented. The first configuration uses plane-parallel (or plano-convex) *Fabry-Perot cavities* with *non-uniform* (or periodic) grid mirrors in order to increase the directivity of the primary source and *shape* the radiated beam. Exciting the cavity with an antenna array presenting a moderate directivity improves the mutual coupling and optimizes the radiation performance. The second configuration uses *arbitrarily shaped 3D homogeneous dielectric lenses*. The design procedure leads to a Monge-Ampere differential equation. The latter has been solved for the first time and the corresponding algorithm is validated successfully at 58.5 GHz.

#### 5. References

- [1] Mini-special issue on "Electromagnetic crystal structures, design, synthesis and applications", *IEEE trans. on MTT*, vol. 47, n°11, Nov. 1999.
- [2] P. de Maagt, R. Gonzalo, Y. C. Vardaxoglou, J.-M. Baracco, "Electromagnetic bandgap antennas and components for microwave and (sub)millimeter wave applications", *IEEE trans. on AP*, vol. 51, n°10, pp. 2667-2677, Oct. 2003.
- [3] A. Ortusi, J.-C. Simon, "Hertzian optics", US Pat. 2,763,860, Sept. 18, 1956.
- [4] G. von Trentini, "Partially reflecting sheet arrays", *IRE trans. on AP*, vol. 4, n°10, pp. 666-671, Oct. 1956.
- [5] E. Ozbay, B. Temelkuran, M. Bayindir, R. Biswas, M. M. Sigalas, G. Tuttle, K. Ho, "Photonic crystals based resonant antenna with a very high directivity", *Millenium Conf. on Antennas and Propagation, AP'2000*, Davos, Switzerland, Session 2A2, April 2000.
- [6] C. Cheype, C. Serier, M. Thévenot, Th. Monédière, A. Reinex, B. Jecko, "An electromagnetic bandgap resonator antenna", *IEEE trans. on AP*, vol. 50, n°9, pp. 1285-1290, Sept. 2002.
- [7] S. Enoch, N. Guérin, G. Tayeb, P. Vincent, "Study of photonic crystal based directive antennas", *24<sup>th</sup> ESTEC antenna workshop on innovative periodic antennas: photonic bandgap, fractal and frequency selective structures*, Noordwijk, The Netherlands, pp. 11-16, June 2001.
- [8] R. Sauleau, Ph. Coquet, T. Matsui, "Low-profile directive quasi-planar antennas based on millimeter wave Fabry-Perot cavities", *IEE proc. Microwaves, Antennas and Propagation*, vol. 150, n°4, pp. 274-278, Aug. 2003.
- [9] R. Sauleau, Ph. Coquet, D. Thouroude, J.-P. Daniel, T. Matsui, "Radiation characteristics and performance of millimeter wave horn fed gaussian beam antennas", *IEEE trans. on AP*, vol. 51, n°3, pp. 378-387, March 2003.
- [10] R. Sauleau, Ph. Coquet, T. Matsui, J.-P. Daniel, "A new concept of focusing antennas using plane-parallel Fabry-Perot cavities with non-uniform mirrors", *IEEE trans. on AP*, vol. 51, n°11, pp. 3171-3175, Nov. 2003.
- [11] A. Hoorfar, J. Zhu, N. Engheta, "Evolutionary synthesis of non-uniform partially reflective surfaces for beam shaping of microstrip antennas", *Intern. Conf. on Electromagnetics in Advanced Applications, ICEAA'03*, Torino, Italy, 8-12 September, 2003.
- [12] R. Sauleau, Ph. Coquet, T. Matsui, "Near-field coupling between a printed antenna and a Fabry-Perot resonator: experimental study of the radiation properties at millimeter wave frequencies", *Microwave and Optical Technology Letters*, vol. 38, n°6, pp. 438-443, Sept. 2003.
- [13] C. A. Fernandes, L. M. Anunciada, "Constant flux illumination of square cells for millimeter-wave wireless communications", *IEEE trans. on MTT*, vol. 49, n°11, pp. 2137-2141, Nov. 2001.
- [14] J. S. Schruben, "Formulation of a reflector-design problem for a lighting fixture", *Journal of the Optical Society of America*, vol. 62, n°12, pp. 1498-1501, 1972.
- [15] B. Chantraine-Barès, R. Sauleau, K. Mahdjoubi, "A new accurate design method of arbitrarily shaped dielectric lens antenna", submitted to *IEEE trans. on AP*, Feb. 2004.
- [16] B. S. Westcott, "Shaped reflector antenna design", Research Studies Press Ltd, Letchworth, England, 1983.